Asian Journal of Chemistry; Vol. 23, No. 5 (2011), 2327-2331

ASIAN JOURNAL OF CHEMISTRY

www.asianjournalofchemistry.co.in

Rare Earth Oxide-Doped Fullerene and Titania Composites and Photocatalytic Properties of Methylene Blue Under Visible Light†

ZE-DA MENG[1], MING-LIANG CHEN[1], FENG-JUN ZHANG[1,2], LEI ZHU[1], JONG-GEUN CHOI[1] and WON-CHUN OH[1,*]

[1]Department of Advanced Materials & Science Engineering, Hanseo University, Seosan-si, Chungnam-do 356-706, South Korea
[2]Anhui Key Laboratory of Advanced Building Materials, Anhui University of Architecture, Hefei 230022, Anhui Province, P.R. China

*Corresponding author: E-mail: wc_oh@hanseo.ac.kr

AJC-9561

Rare-earth oxide-doped fullerene and TiO_2 composites (Y-fullerene/TiO_2) were prepared by a sol-gel method. The composite obtained was characterized by BET surface area measurements, X-ray diffraction, transmission electron microscopy and energy dispersive X-ray analysis. A methylene blue solution under visible light irradiation was used to determine their photocatalytic activity. Excellent photocatalytic degradation of methylene blue solution was observed using the Y-fullerene/TiO_2 composite under visible light.

Key Words: C_{60}, TiO_2, Visible light, Yttrium, Photocatalytic, Methylene blue.

INTRODUCTION

The sun radiates a tremendous amount of energy to the earth in the forms of near-infrared, visible and ultraviolet light. Since the first report of the photoelectrolysis of water by Fujishima and Honda[1], many attempts have been made to convert solar energy into H_2 through the photocatalytic splitting water by semiconductors (*e.g.* TiO_2 and CdS)[2-7].

TiO_2 has excellent photocatalytic properties and applications in medicine, buildings and environmental remediation[8-11]. However, TiO_2 absorbs only UV light with low quantum efficiency owing to its wide band gap (*ca.* 3.2 eV). Ultraviolet light comprises only a small portion (*ca.* 3-5 %) of sunlight, so the development of more efficient of photocatalysts is needed. Considerable effort has been made to modify TiO_2 to develop multifunctional materials and enhance the photocatalytic performance[12]. To develop more efficient photocatalysts, various methods have been used to improve the optical properties of TiO_2 by modifying its band gap, such as doping with other elements, sensitizing with dyes, coating the surface with noble metals or other semiconductors[13-16].

Nanocarbon materials, such as fullerenes and carbon nanotubes, have been studied extensively owing to their unique structural, electrical and mechanical properties[17]. Fullerenes and their derivatives are promising candidates for these applications, owing to their abundant π-electron systems and resulting electron-accumulating properties. Fullerene has attracted extensive attention for its interesting properties due to their delocalized conjugated structures and electron-accepting ability. One of the most remarkable properties of fullerene in the electron-transfer processes is that it can efficiently stimulate rapid photoinduced charge separation and slow charge recombination[18]. Therefore, the combination of photocatalysts and fullerene can provide an ideal system for achieving enhanced charge separation by photoinduced electron transfer.

The surface composition and structure of photocatalysts can greatly influence its activity. Some important results have been achieved by studies of the rare earth oxide-doped TiO_2 composites. Yan *et al.* reported that the photocatalytic activity of TiO_2 increases after adding rare earth elements and a shift in the band gap energy which results in a red shift in the order of $La^{3+} < Pr^{3+} < Nd^{3+} < Y^{3+}$ doped TiO_2, was observed in the solid state UV-vis spectra[19, 20].

Based on these studies, novel photocatalytic materials were prepared. This involves TiO_2 loading on the fullerene surface and further incorporation of Y^{3+} ions on TiO_2 supported fullerene surface.

The surface sol-gel method was used to prepare Y-C_{60} and Y-C_{60}/TiO_2 compounds. In this technique, metal oxides are chemisorbed on a solid substrate modified with surface hydroxyl groups. To examine the synergism induced after adsorbing TiO_2 and Y_2O_3 nanoparticles on the fullerenes surface, the prepared photocatalysts were examined by X-ray diffraction (XRD), surface area (BET) measurements, scanning electron microscopy (SEM) and energy dispersive X-ray

†Presented to the 4th Korea-China International Conference on Multi-Functional Materials and Application.

analysis (EDX). The performance of these new materials were tested under UV illumination for the photocatalytic decolourization of methylene blue (MB, $C_{16}H_{18}N_3S{\cdot}ClH_2O$). Methylene blue is a water-soluble azo dye that is produced in textile, printing, paper manufacturing, as well as in the pulp processing and pharmaceutical industries. It is a major water pollutant and its release into the environment creates considerable problems. Methylene blue was selected because under anaerobic conditions it has the potential to produce more hazardous aromatic amines. In addition, its decolourization is controlled by the effect of the yttrium ion content.

EXPERIMENTAL

Crystalline fullerene [C_{60}] powder of 99.9 % purity from TCI (Tokyo Kasei Kogyo Co. Ltd., Japan) was used as the carbon matrix. Benzene and ethyl alcohol were purchased as reagent-grade from Duksan Pure Chemical Co (Korea) and Daejung Chemical Co. (Korea) and used without further purification unless otherwise stated. Yttrium nitrate [$Y(NO_3)_3$] as a yttrium source for the synthesis of the Y-fullerene compounds was obtained from Daejung Chemicals & Metals Co., Ltd, Korea. The titanium(IV) *n*-butoxide (TNB, $C_{16}H_{36}O_4Ti$) as a titanium source for the preparation of the Y-fullerene/TiO_2 composites was purchased as reagent-grade from Acros Organics (USA). Methylene blue (MB, $C_{16}H_{18}N_3S.Cl{\cdot}3H_2O$) was analytical grade and also purchased from Duksan Pure Chemical Co., Ltd.

Preparation of Y- C_{60}/TiO_2 composites: *m*-Chloroperbenzoic acid (MCPBA, *ca.* 1 g) was suspended in 50 mL benzene, followed by the addition of fullerene [C_{60}] (*ca.* 100 mg). The resulting mixture was heated under reflux in air and stirred for 6 h. After completion, the dark brown precipitates were washed with ethyl alcohol and dried at 323 K. This mixture was heated under reflux in air and stirred at 343 K for 6 h using a magnetic stirrer in a vial. The Y-C_{60} compounds were obtained after heat treatment at 923 K for 1 h.

The Y treated fullerene composites were placed in to a mixing solution of titanium(IV)-*n*-butoxide and benzene with a volume ratio of 3:47. The solutions were then homogenized under reflux at 343 K for 5 h, while being stirred in a vial. After stirring, the solution was transformed into Y-C_{60}/TiO_2 gels, which were heat treatment at 873 K to produce the Y-C_{60}/TiO_2 composites.

Characterization of Y-C_{60}/TiO_2 compounds: XRD (Shimata XD-D1, Japan) was used for crystal phase identification and to estimate the anatase-to-rutile ratio. The XRD patterns were obtained at room temperature using CuK_α radiation. SEM (JOEL, JSM-5200, Japan) was used to observe the surface state and porous structure of the Y-C_{60}/TiO_2 composites. The elemental composition of the Y-C_{60}/TiO_2 composites was examined by EDX.

Photocatalytic tests: A specified quantity of the Y-C_{60}/TiO_2 composites was added to 50 mL a methylene blue solution. The reactor was placed in the dark for 2 h to allow the maximum adsorption of methylene blue molecules to the Y-C_{60}/TiO_2 composites particles. In all experiments, the initial concentration of the methylene blue was 1×10^{-5} mol/L and the amount of the Y-C_{60}/TiO_2 composite was 0.05 g/(50 mL solution). After adsorption, the photodecomposition of the methylene blue solution was performed under visible light in a dark-box to ensure that the reactor was irradiated by a single light source. The visible light source used was an 18W lamp with the main emission wavelength at 360 nm. Visible light irradiation of the photoreactor was performed for 10, 30, 60, 90, 120 and 150 min. The experiments were performed at room temperature. In the process of methylene blue degradation, a glass reactor (bottom area = 20 cm^2) was used and the reactor was placed on a magnetic churn dasher. Samples were then withdrawn regularly from the reactor and the dispersed powders were removed by a centrifuge. The methylene blue concentration in the solution was then determined as a function of the irradiation time from the change in absorbance at a wavelength of 660 nm.

RESULTS AND DISCUSSION

Structure and morphology of composites: Fig. 1 shows the results of EDX examinations of the surface of the Y-C_{60} and Y-C_{60}/TiO_2 compounds. The elemental composition of these samples was analyzed and the characteristic elements were identified. Fig. 1 shows strong Kα and Kβ peaks from Ti at 4.51 and 4.92 keV, whereas a moderate Kα peak for O appears at 0.52 keV[21]. Besides all the above peaks, Y was also observed. Fig. 2 presents the quantitative microanalysis of C, O, Ti and Y as the major elements for the composites by EDX. Table-1 lists the composition ratios of the samples. There were some small impurities, which are believed to have been introduced from the unpurified yttrium nitrate. In the case of most samples, carbon and titanium were present as major elements with small quantities of oxygen in the composite.

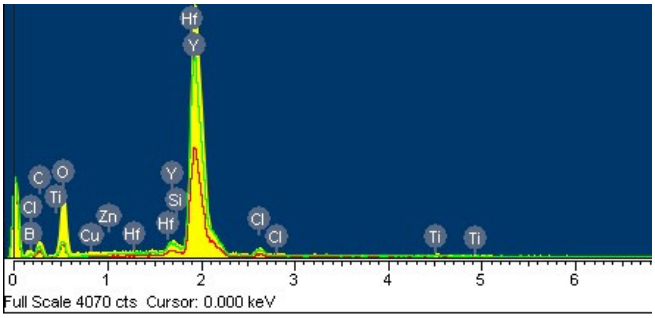

(a)

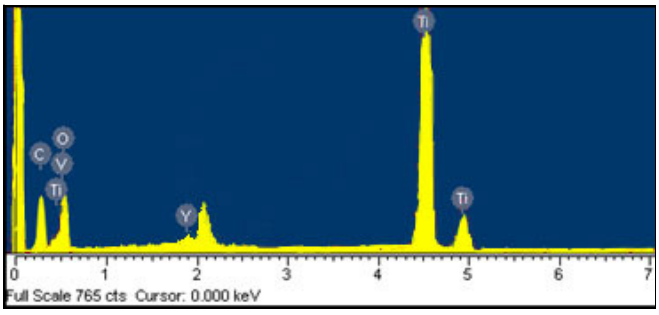

(b)

Fig. 1. EDX elemental microanalysis of the Y-C_{60} (a) and Y-C_{60}/TiO_2 (b) composites

TABLE-1
EDX ELEMENTAL MICROANALYSIS AND
BET SURFACE AREA

Samples	C	O	Y	Ti	Impurity
Y-C_{60}	23.27	28.45	47.11	-	1.17
Y-C_{60}/TiO_2	12.44	36.85	0.56	49.83	0.32

Samples	C_{60}	TiO_2	Y-C_{60}	Y-C_{60}/TiO_2
BET	85.5	17.1	62.0	47.0

Fig. 2 shows SEM images the micro-surface structures and morphology of the Y-C_{60} and Y-C_{60}/TiO_2 compounds. C_{60} and yttrium oxide particles were coated uniformly over the TiO_2 surface, which lead to an increase in nanoparticle size. Zhang *et al.*[22,23] reported that a good dispersion of small particles could provide more reactive sites for the reactants than aggregated particles. The surface roughness appears to be high due to some grain aggregation. Fig. 2(a), (b) and (c) show SEM images of pure TiO_2, Y-C_{60} and Y-C_{60}/TiO_2, respectively. The level of aggregation increased with increasing types of doping. C_{60} and TiO_2 can enhance aggregation.

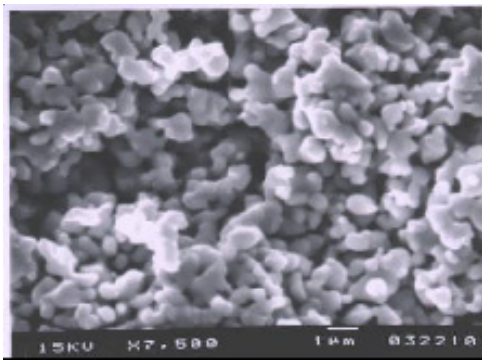

(a)

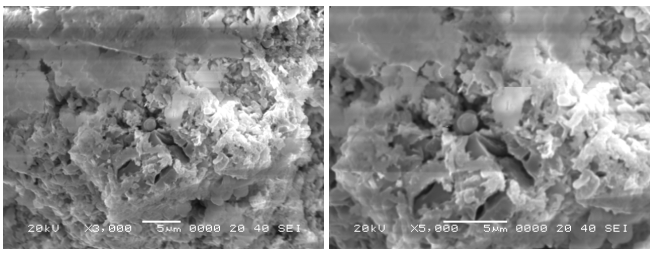

(b)

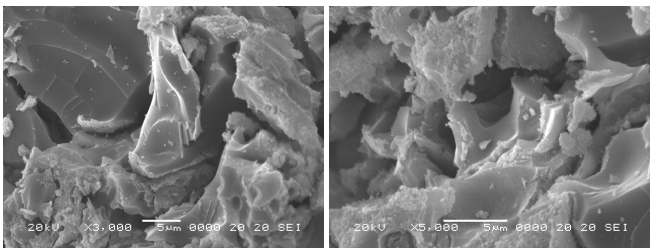

(c)

Fig. 2. SEM images of TiO_2 (a) Y-C_{60} (b) and Y-C_{60}/TiO_2 (c) composites

Fig. 3 shows a TEM image of Y-C_{60} (a) and Y-C_{60}/TiO_2 (b) compounds at different magnifications. The interfacial region of Y-C_{60} and Y-C_{60}/TiO_2 were examined by TEM to obtain more information on the interfacial region of the fullerene crystals and to identify the potential reaction products in this domain. From Fig. 2, large clusters were observed with an irregular agglomerate dispersion of TiO_2. The C_{60} particles were clearly shown from this picture. The light, spherical shape figures in Fig. 3 are C_{60}. The average diameter of C_{60} was estimated to be *ca.* 20 nm. The representative TEM image in Fig. 3 shows that the prepared powders are uniform with some aggregations between particles. Yttrium oxide particles were also observed as black points in the TEM image.

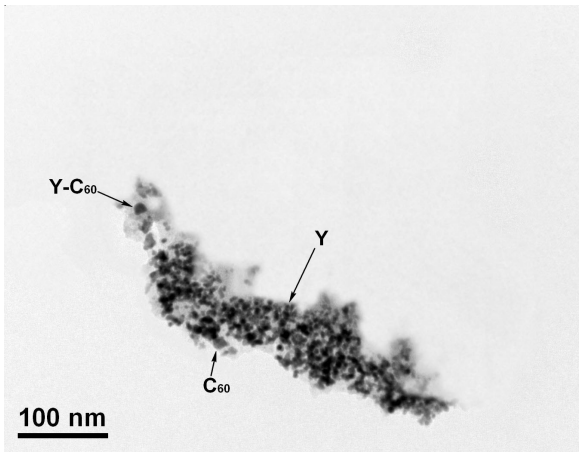

(a)

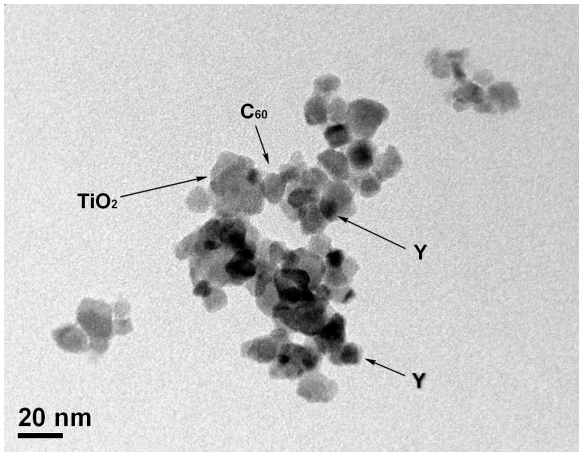

(a)

Fig. 3. TEM images of the Y-C_{60} (a) and Y-C_{60}/TiO_2 (b) composites

Table-1 lists the BET surface areas of the samples. The BET surface areas of pristine C_{60}, TiO_2, prepared Y-C_{60} and Y-C_{60}/TiO_2 were 85, 17.1, 62 and 47 m^2/g, respectively. The TiO_2 and yttrium oxide particles were introduced to the pore of the C_{60}, which decreased the BET surface area. The Y-C_{60} sample had the largest area, which can affect the adsorption reaction. The BET surface area of the photocatalyst Y-C_{60} decreased by 24 % when Y-C_{60} particles were loaded on the TiO_2 support. This is because TiO_2 particles fill the pores of the Y-C_{60} particles, thereby reducing the pore size and pore volume of Y-C_{60} particles[24-26].

Fig. 4 shows XRD patterns of the TiO_2, Y-C_{60} and Y-C_{60}/TiO_2 composites. After heat treatment at 873 K, major peaks were observed at 25.3, 37.9, 48.0, 53.8, 54.9 and 62.5° 2θ, which were assigned to the (101), (004), (200), (105), (211)

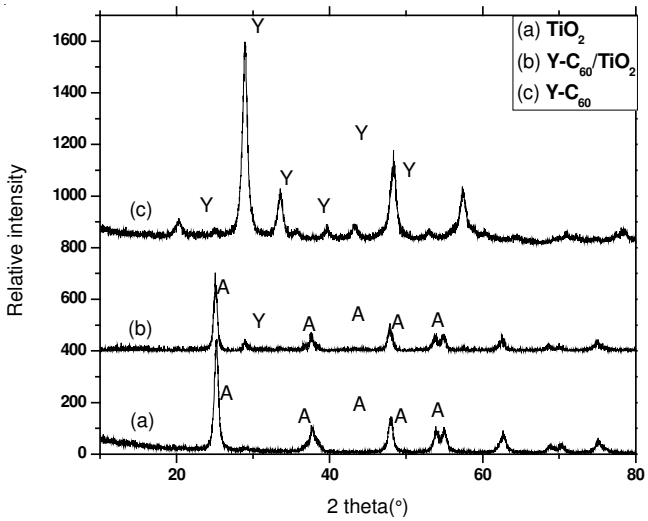

Fig. 4. XRD patterns of TiO_2, Y-C_{60} and Y-C_{60}/TiO_2 composites

and (204) planes of anatase, indicating that the prepared TiO_2 is anatase[27]. These results suggest that Y-C_{60}/TiO_2 is also show pure anatase phase structure under the current preparation conditions. The XRD pattern of Y-C_{60} shows the characteristic peaks of Y_2O_3. Additional Y_2O_3 diffraction peaks for the (211) (222) (400), (332), (134), (440) and (622) planes were observed at 20.4°, 29.24°, 33.76°, 39.8°, 43.74°, 48.90° and 57.6° (2θ), respectively[28-30]. The (222) plane of Y_2O_3 was also observed in the XRD pattern of Y-C_{60}/TiO_2 at 29.3° (2θ). Only one peak for Y_2O_3 was observed in the XRD pattern of Y-C_{60}/TiO_2 due to the low yttrium content.

Degradation of methylene blue solution: Fig. 5 shows the relative concentration of the degraded methylene blue solution by the different samples after irradiation under visible light by different time. There are two steps during degradation of the methylene blue solution. The first step is adsorption, followed by exposure to visible light to degrade the methylene blue solution. Pure TiO_2 had no photocatalytic effect under visible light because of its poor BET surface area, *i.e.* there is little methylene blue adsorption. Y-C_{60} compounds have the highest BET surface area, which can enhance the adsorption of methylene blue. Therefore, Y-C_{60} compounds have the best

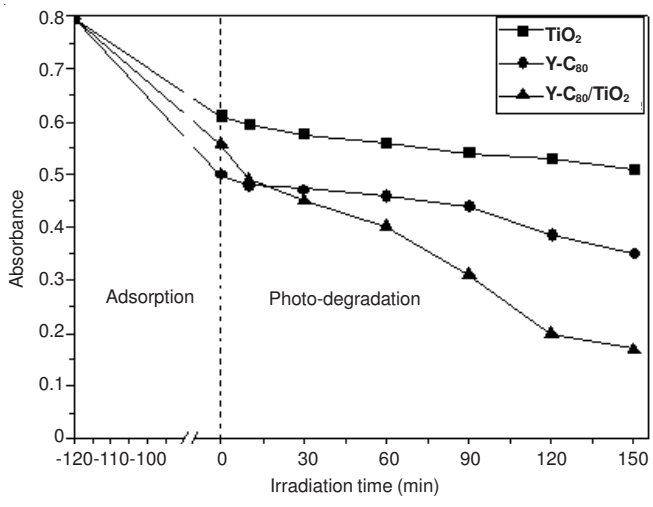

Fig. 5. Absorbance of the methylene blue solution degraded by different samples after irradiation with visible light

adsorption effect in the first step. Fig. 5 shows that Y- C_{60}/TiO_2 has good photocatalytic activity under visible light. This can be attributed to both the effects between photocatalysis of the supported TiO_2, the charge transfer of fullerene and the introduction of yttrium to enhance photogenerated electrons transfer.

In the C_{60} coupled TiO_2 system, the enhancement of the photocatalytic activities was due mainly to the high efficiency of charge separation induced by the synergetic effects of C_{60} and TiO_2. Fig. 6 presents the processes of the photogenerated charge transition during irradiation. When C_{60} was coupled TiO_2, hole and electron pairs were generated and separated on the interface of C_{60} when illuminated by visible light. The level of the conduction band in TiO_2 was lower than the reduction potential of C_{60}[31,32]. Therefore, the photogenerated electron can transfer easily from the conduction band of C_{60} to TiO_2 the molecule due to the interaction between TiO_2 and C_{60}[33]. The synergetic effect of C_{60} and TiO_2 promoted the separation efficiency of photogenerated electron-hole pairs resulting in a high photocatalytic activity of the C_{60}-hybridized TiO_2 samples. In this case, C_{60} improves the activity of TiO_2 under visible light irradiation[34].

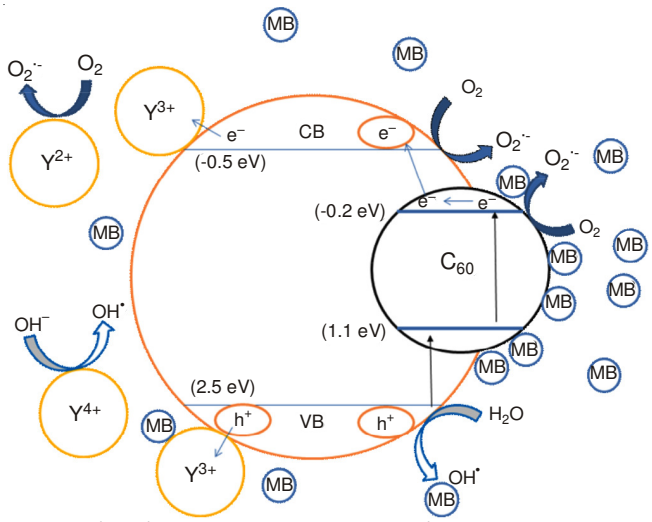

Fig. 6. Schematic diagram of the separation of photogenerated electrons and holes on the Y-C_{60}/TiO_2 interface

Yttrium oxide was used to inhibit electron-hole pair recombination. For this supported catalyst system, charge pair separation was suggested to proceed *via* electron donation from the C_{60}-TiO_2 frame and the electron-accepting role possessed by Y^{3+} ions (electron-trap).

$$Y^{3+} + e^- \rightarrow Y^{2+} \quad (1)\ \text{(electron-trap)}$$

$$Y^{3+} + h + H_2O \rightarrow Y^{4+} + O_2^- + H_2 \quad (2)\ \text{(hole-trap)}$$

Another possible pathway may occur by accepting C_{60}-TiO_2 as an electron-delocalizing region. This probable route is relatively rare compared to the electron-donating task of the C_{60}-TiO_2 system due to the limited number of C_{60} sites in its structure.

In both situations, the unstable nature of Y^{2+} and Y^{4+} ions initiates the transfer of trapped charges to the interface by the

following equations. Highly reactive superoxide ions ($O_2^{\bullet-}$) may also form hydroxyl radicals in the acidic media.

$$Y^{2+} + O_2 \rightarrow Y^{3+} + O_2^{\bullet-} \quad (3)$$

$$Y^{4+} + OH^- \rightarrow Y^{3+} + OH^{\bullet} \quad (4)$$

Oxidative degradation of azo dyes generally occurs by the attack of hydroxyl radicals, which are known as highly reactive electrophilic oxidants[35-38].

$$\text{I - MB} + OH^{\bullet} + O_2^{\bullet-} \rightarrow \text{I} + \text{aliphatic compounds} + OH^{\bullet} \rightarrow CO_2 + H_2O + \text{inorganic} \quad (5)$$

(I: adsorption site)

Y-C_{60}/TiO_2 has a good photo-degradation effect due to the the high efficiency of charge separation induced by the synergetic effect of C_{60} and TiO_2 and the inhibition of the electron-hole pair recombination of yttrium.

Conclusion

This paper reports the preparation and characterization of TiO_2, Y-C_{60} and Y-C_{60}/TiO_2 composites. The BET surface area of pristine C_{60} was higher than that of the Y-C_{60}/TiO_2. X-ray diffraction revealed the Y_2O_3 structure and anatase. Transmission electron microscopy showed that TiO_2 particles with some agglomerates were dispersed over the surface of C_{60} together with Y_2O_3 particles. The Y-C_{60}/TiO_2 composite showed the best photocatalytic degradation activity of the methylene blue solution under visible light irradiation. This was attributed to the three different effects between the photocatalytic reaction of the supported TiO_2, decomposition of the organometallic reaction by the Y compound and the energy transfer effects of fullerene, such as electrons and light.

REFERENCES

1. F.J. Zhang, M.L. Chen, K. Zhang and W.C. Oh, *Bull. Korean. Chem. Soc.*, **31**, 133 (2010).
2. W.X. Dai, X. Chen, X.P. Zheng, Z.X. Ding, X.X. Wang, P. Liu and X.Z. Fu, *ChemPhysChem.*, **10**, 411 (2009).
3. A.L. Linsebigler, G.Q. Lu and J.T. Yates, *J. Chem. Rev.*, **95**, 735 (1995).
4. M. Mrowetz, W. Balcerski, A.J. Colussi and M.R. Hoffmann, *J. Phys. Chem. B*, **108**, 17269 (2004).
5. J.C. Yu, J.W. Yu, H.Z. Jiang and L. Zhang, *Chem. Mater.*, **14**, 3808 (2002).
6. E. Bae and W. Choi, *Environ. Sci. Technol.*, **37**, 147 (2003).
7. J.C. Kim, J.K. Choi, Y.B. Lee, J.H. Hong, J.I. Lee, J.W. Yang, W.I. Lee and N.H. Hur, *Chem. Commun.*, **48**, 5024 (2006).
8. H.G. Kim, D.W. Hwang and J.S. Lee, *J. Am. Chem. Soc.*, **126**, 8912 (2004).
9. U.M.K. Shahed, M. Al-Shahry and I.B. William Jr., *Science*, **297**, 2243 (2002).
10. M.L. Chen, F.J. Zhang, K. Zhang, Z.D. Meng and W.C. Oh, *Elas. Cpmp.*, **45**, 25 (2010).
11. Z.D. Meng, K. Zhang and W.C. Oh, *J. Korean Cry. Grow. Cry. Tech.*, **19**, 268 (2009).
12. Y. Yang, X. Li, J. Chen and L. Wang, *J. Photochem. Photobiol. A: Chem.*, **163**, 517 (2004).
13. T. Okazaki, K. Suenaga, Y.F. Lian, Z.N. Gu and H. Shinohara, *J. Chem. Phys.*, **113**, 9593 (2000).
14. A. Fujishima and K. Honda, *Nature*, **238**, 37 (1972).
15. Z. Zou, J. Ye, K. Sayama and H. Arakawa, *Nature*, **414**, 625 (2001).
16. S.U.M. Khan, M. Al-Shahry and W.B. Ingler Jr, *Science*, **297**, 2243 (2002).
17. J.J. Davis, H.A.O. Hill, A. Kurz, A.D. Leighton and A.Y. Safronov, *J. Electroanal. Chem.*, **429**, 7 (1997).
18. A. Szucs, A. Loix, J.B. Nagy and L. Lamberts, *J. Electroanal. Chem.*, **397**, 191 (1995).
19. Q.L. Wang, G.D. Lian and E.C. Dickey, *Acta Mater.*, **52**, 809 (2004).
20. H.R. Zhang, K.Q. Tan, H.W. Zheng, Y.Z. Gu and W.F. Zhang, *Mater. Chem. Phys.*, **125**, 156 (2011).
21. W.C. Oh, A.R. Jung and W.B. Ko, *Mater. Sci. Eng.*, **C29**, 1338 (2009).
22. F.J. Zhang, J. Liu, M.L. Chen and W.C. Oh, *J. Korean Ceram. Soc.*, **46**, 263 (2009).
23. X.W. Zhang, M.H. Zhou and L.C. Lei, *Carbon*, **43**, 1700 (2005).
24. F.J. Zhang, M.L. Chen, K. Zhang and W.C. Oh, *Bull. Korean Chem. Soc.*, **31**, 133 (2010).
25. W.C. Oh, J.H. Son, F.J. Zhang and M.L. Cheng, *J. Korean. Ceram. Soc.*, **46**, 1 (2009).
26. F.J. Zhang and W.C. Oh, *Asian J. Chem.*, **23**, 372 (2011).
27. M.A. Barakat, H. Schaeffer, G. Hayes and S. Ismat-Shah, *Appl. Catal. B: Environ.*, **57**, 23 (2005).
28. J. Lin and J.C. Yu, *J. Photochem. Photobiol. A: Chem.*, **116**, 63 (1998).
29. A.A. Ismail, *Appl. Catal. B: Environ.*, **58**, 115 (2005).
30. A.N. Okte and O. Yilmaz, *Appl. Catal. B. Environ.*, **85**, 92 (2008).
31. R.C. Haddon, A.F. Hebard, M.J. Rosseinsky and D.W. Murphy, *Nature*, **350**, 320 (1991).
32. C.J. Brabec, N.S. Sariciftci and J.C. Hummelen, *Adv. Funct. Mater.*, **11**, 15 (2001).
33. Y.P. Sun, R. Gudure, G.E. Lawson, J.E. Mullins, Z. Guo, J. Quinlan, C.E. Bunker and J.R. Gord, *J. Phys. Chem. B*, **104**, 4625 (2000).
34. K. Yamamoto, M. Saunders, A. Khong, R.J. Gross, J.M. Grayson, M.L. Gross, A.F. Benedetto and R.B. Weisman, *J. Am. Chem. Soc.*, **121**, 1591 (1999).
35. M. Stylidi, D.I. Kondarides, X.E. Verykios, *Appl. Catal. B: Environ.*, **47**, 189 (2004).
36. M. Gratzel and R.F. Howe, *J. Phys. Chem.*, **94**, 2566 (1990).
37. J. Soria, J.C. Conesa, V. Augugliaro, L. Palmisano, M. Schiavello and A. Sclafani, *J. Phys. Chem.*, **95**, 274 (1991).
38. I. Nakamura, N. Negishi, S. Kutsuna, T. Ihara, S. Sugihara and K. Takeuchi, *J. Mol. Catal. A: Chem.*, **161**, 205 (2000).